Nuclear Science and Techniques (2026) 37:17
https://doi.org/10.1007/s41365-025-01843-9

Conceptual design of the subcritical assemblies based on the PWR conventional fuel using DRAGON and DONJON codes

S. Abedi[1] · S. Z. Kalantari[1] · J. Mokhtari[2] · M. H. Choopan Dastjerdi[2] · A. Asgari[2]

Received: 26 April 2024 / Revised: 15 August 2024 / Accepted: 13 September 2024 / Published online: 9 December 2025

Abstract
Subcritical reactors (SCRs) or subcritical assemblies (SCAs) are the main infrastructure for designing power reactors. These reactors are widely used for training and research because of their high level of inherent safety. The objective of this study is to design a subcritical reactor using a pressurized water reactor (PWR) conventional fuel following two safety points. In the first approach, deeply placed SCR cores with an infinite multiplication factor (k_{∞}) of less than unity were identified using the DRAGON lattice code. In the second approach, subcritical reactor cores with an effective multiplication factor (k_{eff}) of less than unity were determined by coupling the cell calculations of the DRAGON lattice code and core calculations of the DONJON code. For the deeply subcritical reactor design, it was found that the reactor would remain inherently subcritical while using fuel rods with ^{235}U enrichment of up to 0.9%, regardless of the pitch of the fuel rods. In the second approach, the optimal pitches (1.3 to 2.3 cm) were determined for different fuel enrichment values from 1 to 5%. Subsequently, the k_{eff} was obtained for a fuel rod arrangement of 8×8 to 80×80, and the states in which the reactor would be subcritical were determined for different fuel enrichments at the corresponding optimal pitch. To validate the models used in the DRAGON and DONJON codes, the k_{eff} of the Isfahan Light Water Subcritical Reactor (LWSCR) was experimentally measured and compared with the results of the calculations. Finally, the effects of fuel and moderator temperature changes were investigated to ensure that the designed assemblies remained in the subcritical state at all operational temperatures.

Keywords Subcritical reactor design · Multiplication factor · Light water subcritical reactor (LWSCR) · Moderator temperature coefficient (MTC) · Fuel temperature coefficient (FTC)

1 Introduction

A nuclear reactor is a system in which the chain reaction of nuclear fission is initiated, maintained, and controlled. SCRs are a type of research reactor in which fission occurs without reaching criticality. The content of fissile material and supplementary materials, such as the structure of the fuel meat, reflector, moderator, and fuel clad, is insufficient to achieve a self-sustaining chain reaction in an SCR. The chain reaction in such reactors is initiated and maintained using an external neutron source. The goals for the design and use of SCRs are diverse, including research and training, computational code benchmarking, cross-section measurements, detector calibration, spent fuel conversion, and the development of advanced measurement techniques [1–11]. Although other research reactors are capable of producing a high neutron flux for irradiation experiments such as radioisotope production, neutron radiography, neutron activation analysis, and material characterization, the main drawback of this type of research reactor is its lower neutron flux compared to other research reactors, which restricts some of the aforementioned applications [12–25]. The stockholders of SCRs are students, trainees, and researchers who gain experience and learn how to calculate reactor physics parameters.

One of the important parameters in the design of nuclear reactors is the effective multiplication factor, k_{eff}, which is the ratio of the number of neutrons produced by fission

✉ J. Mokhtari
jvmokhtari@aeoi.org.ir

✉ M. H. Choopan Dastjerdi
mdastjerdi@aeoi.org.ir

[1] Department of Physics, Isfahan University of Technology, Isfahan 841568311, Iran

[2] Reactor and Nuclear Safety Research School, Nuclear Science and Technology Research Institute, Isfahan, Iran

in one generation to the number of neutrons lost through absorption and leakage in the previous generation. The design of the reactor core from various aspects of safety and economy, which is based on the choice and assessment of the behavior of different fuels and moderators, has been an attractive topic in the design of research and power reactors [26–31]. For an infinite reactor core size, there is no neutron leakage. For such a core, the infinite multiplication factor, k_{∞}, is the ratio of the number of neutrons resulting from fission in each generation to the number of neutrons absorbed in the previous generation. If k_{eff} is less than unity ($k_{\text{eff}} < 1$), the nuclear reactor is called subcritical. In the case of SCRs, if k_{∞} is less than unity, the reactor is called a deeply SCR [32–35]. It is worth noting that a deeply SCR remains subcritical under any conditions and cannot reach criticality by adding more similar fuel rods. Owing to their inherent safety, deep subcritical reactors are very useful for teaching reactor physics parameters, such as the measurement of diffusion length, Fermi age, migration area, effective multiplication factor, flux distribution, asymptotic region, thermal utilization factor, reflector saving, buckling, effective fraction of delayed neutrons, decay constant, and the average half-life of delayed neutrons [35]. Other SCRs can remain subcritical with geometric constraints but can reach a critical state by adding more similar fuel rods [36]. The IAEA determined the main numerical criterion $k_{\text{eff}} = 0.98$ to ensure the nuclear safety of the SCR [37].

There are two groups of SCRs: One group uses radioisotope neutron sources, such as californium-252 or Americium-Beryllium, to initiate and maintain the chain reaction, and the second group uses a particle accelerator, called an accelerator-driven subcritical reactor (ADSCR). Most ADSs designs propose a high-intensity proton accelerator with an energy of 1 GeV directly attached to the spallation target or spallation neutron source [34, 37].

Some of the subcritical assemblies around the world include: Yalina-Booster subcritical assembly, Subcritical Assembly in Dubna (SAD), Delphi subcritical assembly, Jordan Subcritical Assembly (JSA), Universidad Autonoma de Zacatecas Subcritical Reactor, VR-2 Reactor at the Faculty of Nuclear Sciences, Isfahan Light Water Sub-Critical Reactor (LWSCR), CTU in Prague [34, 36–39].

The Isfahan LWSCR is a thermal reactor that uses natural metal uranium fuel elements. The effective multiplication factor of this reactor was less than unity. The Isfahan LWSCR does not have any control or protection systems for reactor operations. A total of 240 fuel rods were arranged in a hexagonal lattice. All fuel rods are the same, and the diameter and active length of the fuel rods are 3.3 cm and 100 cm, respectively. Each fuel rod is composed of five natural metal uranium fuel slugs with a length of 20 cm [39]. The Jordan Subcritical Reactor (JSA) is an SCRs with UO_2 low-enriched uranium (LEU) fuel and a light water moderator designed based on PWR reactor fuel. In this reactor, the core consists of 313 fuel rods made of UO_2 (3.4 wt% of ^{235}U) with M5 cladding, arranged in the form of a quadrangular with a pitch of 1.91 cm. The k_{eff} of the JSR was 0.9592 [34]. Monte Carlo modeling has also been used to analyze the criticality, reactivity, neutron flux, and spectrum of the JSR. Neutronic design parameters, including the effective multiplication factor, optimal fuel lattice pitch, optimal moderator level, optimal reflector thickness, and neutron flux distribution in the JSR, were studied. Persson et al. analyzed the reactivity of the Yalina subcritical assembly using the slope fit, Sjöstrand, and source jerk methods. They compared their results with Monte Carlo simulations and demonstrated a strong correlation with the slope fit results, indicating the reliability of the method for reactivity analysis in subcritical systems [38–41]. The criticality and flux of a subcritical assembly were studied computationally to investigate the effects of different fuel, moderator, and reflector types. That study found that subcritical assemblies with UO_2 fuel have larger reactivity coefficients, lower criticality, and lower average total neutron flux than those with metal U fuel. Furthermore, the assemblies using both fuel types are inherently safe owing to the negative temperature coefficient of the fuel and moderator, which ensures the safety of the reactor [34].

A feasibility study of power upgrading in the SAD was conducted using a Monte Carlo simulation. The assembly was loaded with mixed oxide fuel (MOX) fuel, and the study concluded that the reactor could be operated at a power level of 100 kW while remaining subcritical with a k_{eff} of 0.972 [35].

The DRAGON lattice code and DONJON full-core simulation code have been actively developed since 1990. A lattice code is the primary software component for describing the behavior of neutrons in a nuclear reactor with a deterministic numerical solution of the Boltzmann transport equation. The DRAGON lattice code was developed over a unit cell, which is a small spatial 2D/3D region of the reactor that can be repeated by symmetry or translation. The DONJON code is a set of independent modules that simulates the 3D neutronic behavior of a nuclear reactor by solving the neutron diffusion equation or simplified Pn (SPn) equation. The coupling of these codes can be applied to simulate and calculate the reactor physics parameters, simplified thermo-hydraulics behavior, 3D neutron kinetics parameters, reactor fuel cycle, pin-flux reconstruction, and boron critical control. The DRAGON and DONJON codes have been validated in various references [42–48].

In this study, based on the safety criteria, we attempted to determine the best arrangement of the subcritical reactor core for various LEU fuels of PWR conventional uranium oxide fuel using deterministic calculations. In addition, a deeply subcritical core with a maximum k_{eff} was introduced for the mentioned fuel for the first time by considering

the weight of the core and economic issues. Furthermore, various square core arrangements with different LEU fuel enrichments (up to 5 wt% ^{235}U enrichment with 0.2% intervals) were modeled, and the best arrangement for each enrichment was selected based on the IAEA safety suggestions. To ensure the accuracy and reliability of the applied models in the DRAGON and DONJON codes, the Isfahan LWSCR was modeled with these codes, and k_{eff} was compared with experimental results.

2 Material and methods

A small tank with a diameter of 140 cm and height of 200 cm that has been filled with light water is considered as the reactor tank to calculate the k_{eff}. The fuel, clad, and moderator specifications are considered similar to those of the NuScale reactor, as shown in Table 1 [49].

The DRAGON lattice code and DONJON full-core simulation code according to the following steps have been used to recommend subcritical cores for different fuel enrichments. To reduce the complexity of the problem, the fuel rod design was eliminated, and the standard PWR fuel was considered. Two approaches were followed: The first was the determination of a deeply subcritical core with maximum k_{eff}, and the second was the determination of the number of fuel rods that lead to a subcritical state of the reactor for various fuel enrichments up to 5 wt% of U-235 by coupling the DRAGON and DONJON codes. All calculations, except for the calculation of the temperature coefficients of reactivity, were performed at room temperature.

The WIMSD-IAEA-69 group microscopic cross-section library was used in the macroscopic cross-section calculations of the DRAGON code. The WIMSD-IAEA-69 group cross-section library encompasses a comprehensive compilation of over 170 isotopes derived from meticulously selected evaluated nuclear data files. Extensive validation procedures were conducted across a spectrum of more than 200 benchmark cases to ensure the accuracy and reliability of the library [44, 50, 51].

Table 1 Fuel and clad properties

Parameter	Value
Fuel	UO_2
Fuel density (g/cm^3)	10.5
Clad material	M5 (Nb 0.01, O 0.00135, Fe 0.00038, Zr 0.98827 wt%)
Clad density (g/cm^3)	8.902
Moderator	Light water
Moderator density (g/cm^3)	0.998207
Fuel meat diameter (cm)	0.81153
Gap thickness (cm)	0.00826
Clad inside diameter (cm)	0.82804
Clad outside diameter(cm)	0.94996

A two-dimensional square cell with a fuel rod at its center was simulated in the GEO module of the DRAGON code (see Fig. 1a). The atomic density and temperature of each isotope were defined in the LIB module. This module interpolates the required data from a microscopic cross-section library. The SYBYLT module, which uses the collision probability method, was used to solve the integral form of the transport equation. The SHI module was used for self-shielding calculations. This module performs fuel self-shielding calculations using the Stammler method. In addition, the ASM module was used to generate the collision probability matrix. The FLU module was used to calculate the multi-group neutron flux and infinite multiplication factor. Finally, the EDI module was applied to generate homogenized cross sections. Homogenized cross sections were used in the DONJON code to calculate the effective multiplication factor. Different arrangements of fuel rods, from 8×8 to 80×80, were simulated in the DONJON code using the GEO module. For example, a 16×16 array is shown in Fig. 1b. The three-dimensional TRIVAT module was used for numerical discretization and tracking of the reactor geometry. The TRIVAA module was also used because the purpose was to calculate a set of system matrices, taking into account the "Tracking" information obtained earlier. Finally, the FLPOW module was used to calculate the effective multiplication factor.

The effective multiplication factor was calculated in terms of different pitches from 1 to 3 cm to obtain the optimal pitch, and their diagrams were drawn. The pitch with the maximum effective multiplication factor was considered the optimal pitch. The arrangement of fuel rods and temperature coefficient were calculated at the optimal pitch for different fuel enrichments (1% to 5 wt% of ^{235}U at 0.2% intervals).

To obtain the feedback of the moderator and fuel temperature, k_{eff} was calculated at different fuel and moderator temperatures. The temperature coefficient of reactivity (α) was calculated using Eq. (1):

$$\alpha = \frac{\Delta\rho}{\Delta T} = \frac{\frac{k_{\text{eff}}^{\text{final}} - k_{\text{eff}}^{\text{initial}}}{k_{\text{eff}}^{\text{final}} \times k_{\text{eff}}^{\text{initial}}}}{T^{\text{final}} - T^{\text{initial}}}, \tag{1}$$

where $\Delta\rho$ is the change in reactivity associated with the change in the moderator/fuel temperature (ΔT). k_{eff} is the effective multiplication factor, and T is the moderator/fuel temperature. For the moderator feedback, a temperature range of 293–373 K was considered, whereas for the fuel feedback, a temperature range of 293–1573 K was

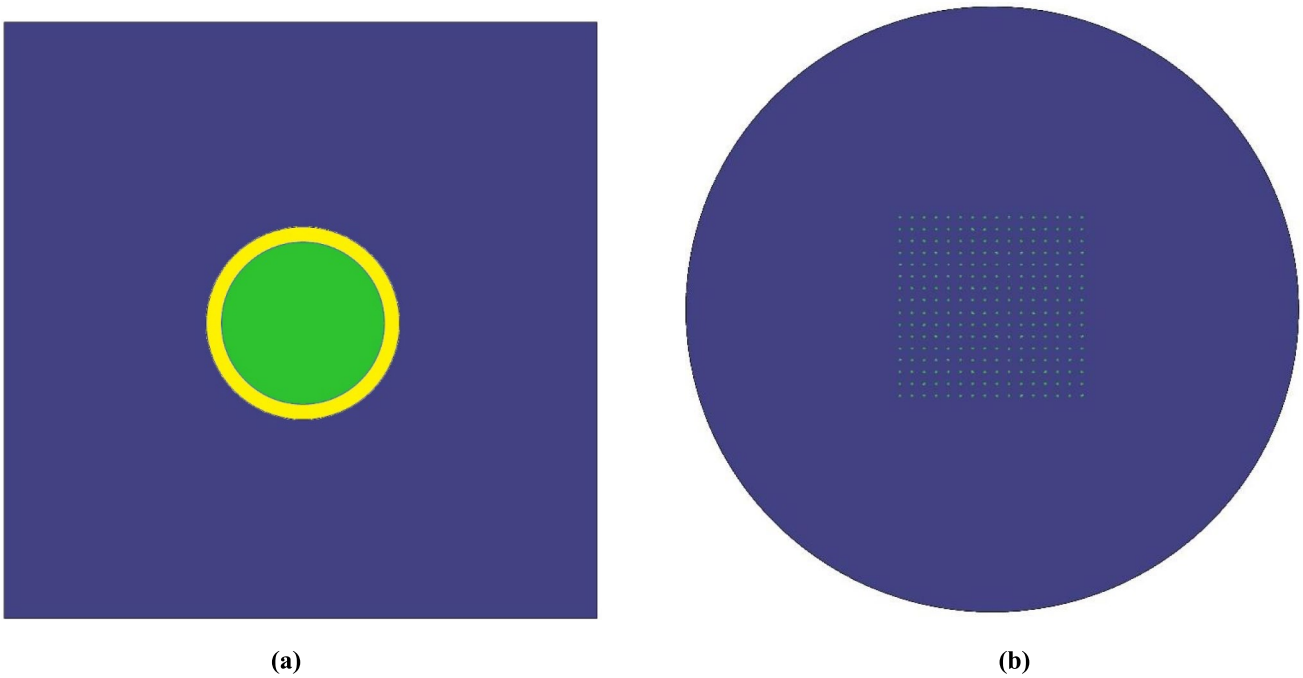

Fig. 1 (Color online) **a** Top view of a fuel rod and **b** Top view of a 16×16 array of fuel rods

considered. Furthermore, the average moderator and fuel temperature coefficients of reactivity were calculated.

3 Results and discussion

3.1 Validation of deterministic codes

This research was conducted at the Esfahan Nuclear Technology Center (ENTC), where a light water subcritical reactor (LWSCR) is in operation. Therefore, the available experimental data from this research reactor were used to benchmark the applied models in the DRAGON and DONJON codes. A general description of the Esfahan LWSCR is presented in Table 2 [39]. The side and top views of the Esfahan LWSCR are shown in Fig. 2. As shown, the natural metal uranium fuel elements are arranged in a hexagonal lattice shape in the Isfahan LWSCR. All 240 fuel rods have the same geometrical shape and material, and the diameter and active length are 3.3 cm and 100 cm, respectively. Each fuel rod was composed of five fuel slugs with the same diameter and 20 cm in length.

The Isfahan LWSCR was modeled using the DRAGON and DONJON codes (see Fig. 3). The effective multiplication factor and average reactivity coefficient in the temperature range of 293–353K for the aforementioned arrangement were compared with the experimental results. The results of the measured values of the effective multiplication factor and average reactivity coefficient are compared with the calculated values of the coupling of the DRAGON and DONJON codes in Table 3. As can be seen, the calculated result of the deterministic model is in good agreement with the measured value of the effective multiplication factor in the Isfahan LWSCR.

Table 2 General Description of Isfahan LWSCR [34]

Characteristic	Description
Fuel	Natural metallic uranium
Number of fuel slug in each rod	5
Diameter/Height of fuel slug (mm)	30/100
Number of fuel rods	240
Moderator	Light water
Cladding	Nickel
Core height/Radius (m)	1/0.36
Tank material	Steel
Tank height/Radius (m)	2/0.7

3.2 Design of a deeply subcritical core

The relationship between k_∞ and the lattice pitch for natural fuels up to 5 wt% of ^{235}U enrichment in 0.25% intervals is shown in Fig. 4. As can be seen, k_∞ has a maximum or optimum value at a particular lattice pitch, which decreases steadily if it moves to a smaller or larger lattice

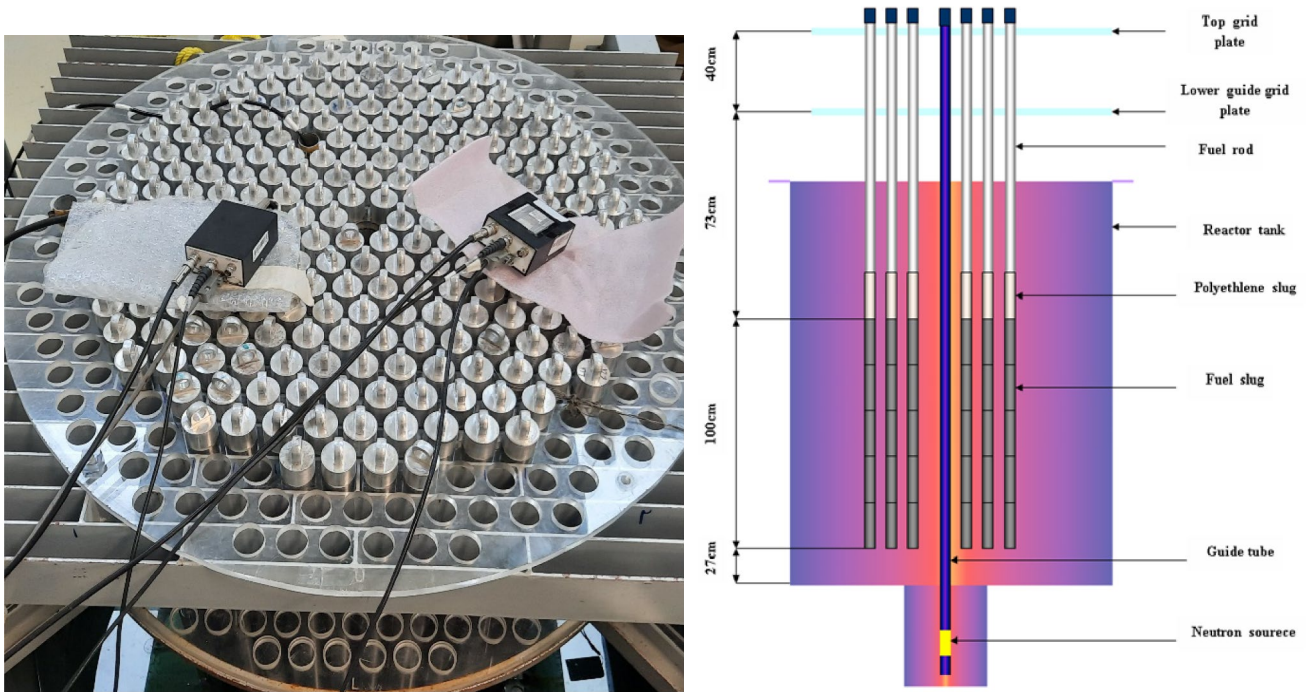

Fig. 2 (Color online) **a** Top photographic view and **b** Side Schematic view of Isfahan LWSCR

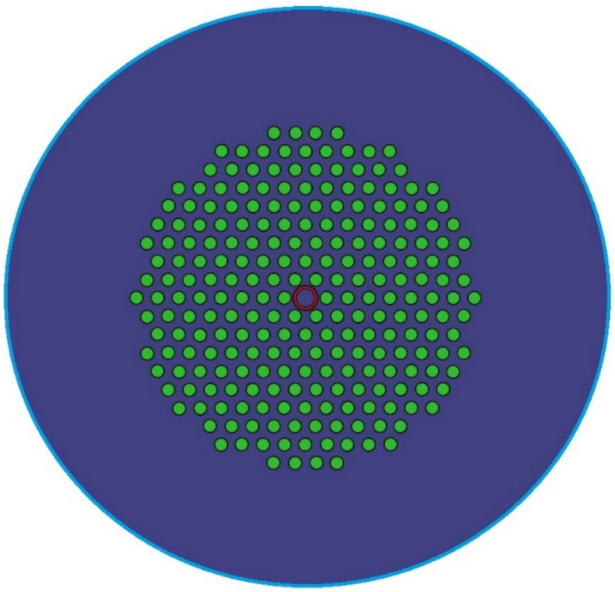

Fig. 3 (Color online) Top view of the simulated reactor core

pitch. If the lattice pitch is higher than the optimal value, the extra moderator will absorb too many neutrons before they have a chance to be absorbed in the fuel, and thus, k_{∞} will decrease. This region is known as an unsafe region in the design of reactors and is called the over-moderated region. In this region, an increase in temperature leads to an increase in the distance between the moderator molecules; therefore, the absorption of neutrons in the moderator decreases, and the multiplication factor increases. However, if the lattice pitch is chosen below the optimal value, the distance for the thermalization of neutrons is small, and more neutrons are absorbed in the U-238 resonances before thermalization. This region is known as a safe region in the design of reactors and is called the under-moderated region. In this region, an increase in temperature leads to an increase in the distance between the moderator molecules; therefore, the slowing down of neutrons decreases, and as a result, the multiplication factor decreases. According to Fig. 4, increasing the fuel

Table 3 Comparison of measured and calculated values of k_{eff} and α for the Isfahan LWSCR

	LWSCR SAR [39]	Computational results	Relative error %
k_{eff}	0.847	0.845	0.24
$\alpha_{293\text{-}353}$ (pcm/K)	−3.86	−4.02	4.1

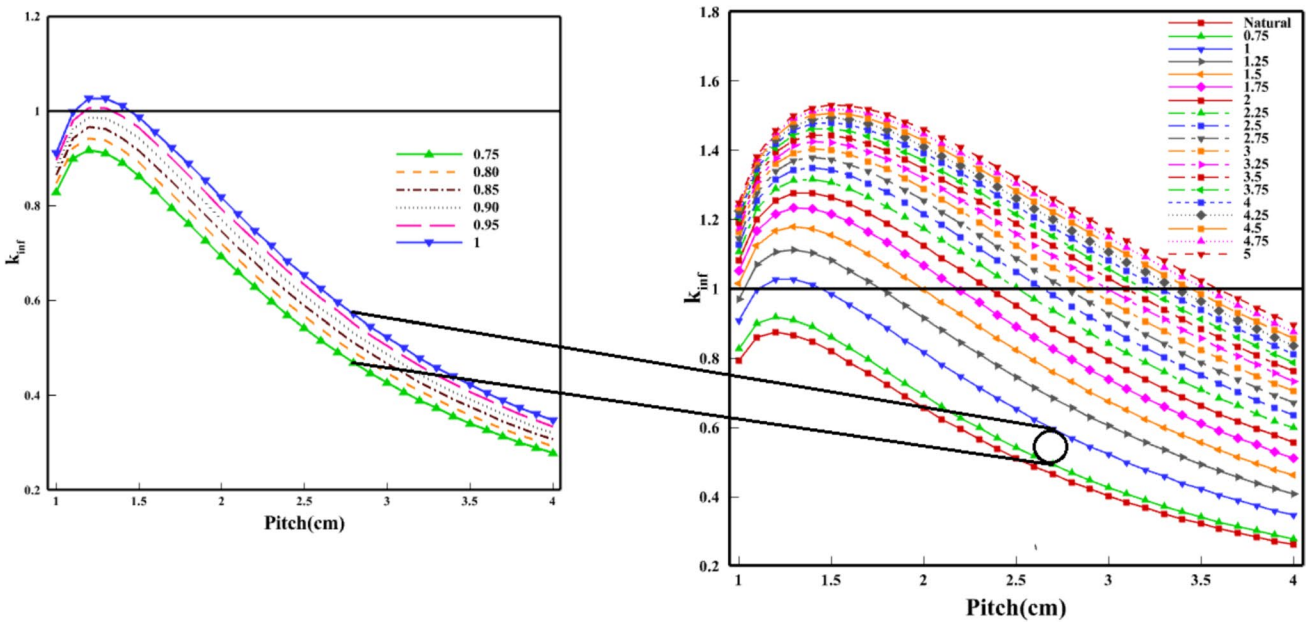

Fig. 4 (Color online) The k_{inf} in terms of lattice pitch for natural up to 5 wt% enriched fuels

enrichment leads to an increase in k_{∞} and the optimum lattice pitch. At higher fuel enrichments, the increase in k_{∞} is smaller. To accurately determine the maximum fuel enrichment at which the reactor remains inherently subcritical ($k_{\infty} < 1$), the fuel enrichment was increased in 0.05% intervals from 0.75 to 1 wt% of ^{235}U enrichment, as shown on the left side of Fig. 4. As can be seen, using fuels with enrichment up to 0.9%, regardless of the fuel rod pitch, the reactor remains inherently subcritical. Therefore, fuel with an enrichment of 0.9 wt% ^{235}U was chosen to design a deeply subcritical reactor with a maximum k_{eff}.

To determine the maximum k_{eff} of the selected design of the deeply subcritical reactor (0.9 wt% of ^{235}U enrichment), fuel rods with different arrangements from 20 × 20 to 90 × 90 for different fuel rod heights from 10 to 120 cm at optimal fuel rod pitch were simulated in a reactor tank with a diameter of 140 cm and height of 200 cm. The simulation results are shown in Fig. 5. As shown in this figure, increasing the height of the fuel rods led to an increase in k_{eff}, but the growth rate decreased with an increase in the height of the fuel rods, with minimal noticeable growth beyond 60 cm. By increasing the number of fuel rods, the k_{eff} also increased. However, the growth rate decreased as the number of fuel rods increased. For instance, when the arrangement of fuel rods is increased from 60 × 60 to 70 × 70, 70 × 70 to 80 × 80, and 80 × 80 to 90 × 90, the value of k_{eff} increases to 2.6%, 1.8%, and 1.2%, respectively. Considering the core weight and economic factors, a core consisting of 80 × 80 fuel rods with a height of 60 cm has a k_{eff} of 0.874 and can be selected as a deeply subcritical reactor.

3.3 Design of an enriched subcritical reactor

This section aims to introduce diverse square subcritical core configurations with varying LEU fuel enrichments of up to 5 wt% ^{235}U enrichment with 2% intervals. The most suitable core for each enrichment was determined based on the IAEA safety recommendations ($k_{eff} < 0.98$).

To obtain the optimal length of the reactor core for different fuel enrichment levels from 1 to 5 wt% of ^{235}U, fuel rods with a 20 × 20 arrangement and a pitch of 2 cm for different heights from 10 to 120 cm were simulated inside the reactor tank. As shown in Fig. 6, an increase in both the height and enrichment of the fuel rods leads to an increase in k_{eff}. However, the rate of increase decreases as the height and enrichment of the fuel rods increase. In addition, the k_{eff} value evidently increases by 5.07%, 2.02%, and 1.01% as the core height increases from 40 to 60 cm, 60 to 80 cm, and 80 to 100 cm, respectively. Therefore, the variations in k_{eff} were more pronounced for core heights below 60 cm than for heights exceeding 60 cm. As a result, a core height of 60 cm was deemed suitable for reactor fuel enrichment ranging from 1 to 5 wt% of ^{235}U.

To find the optimal enriched square subcritical configurations that satisfy the IAEA recommendation for the design of subcritical reactors, the k_{eff} versus the reactor lattice pitch was calculated for 1–5 wt% ^{235}U enrichment with 0.2% intervals and the core arrangements from 8 × 8 to 80 × 80 fuel

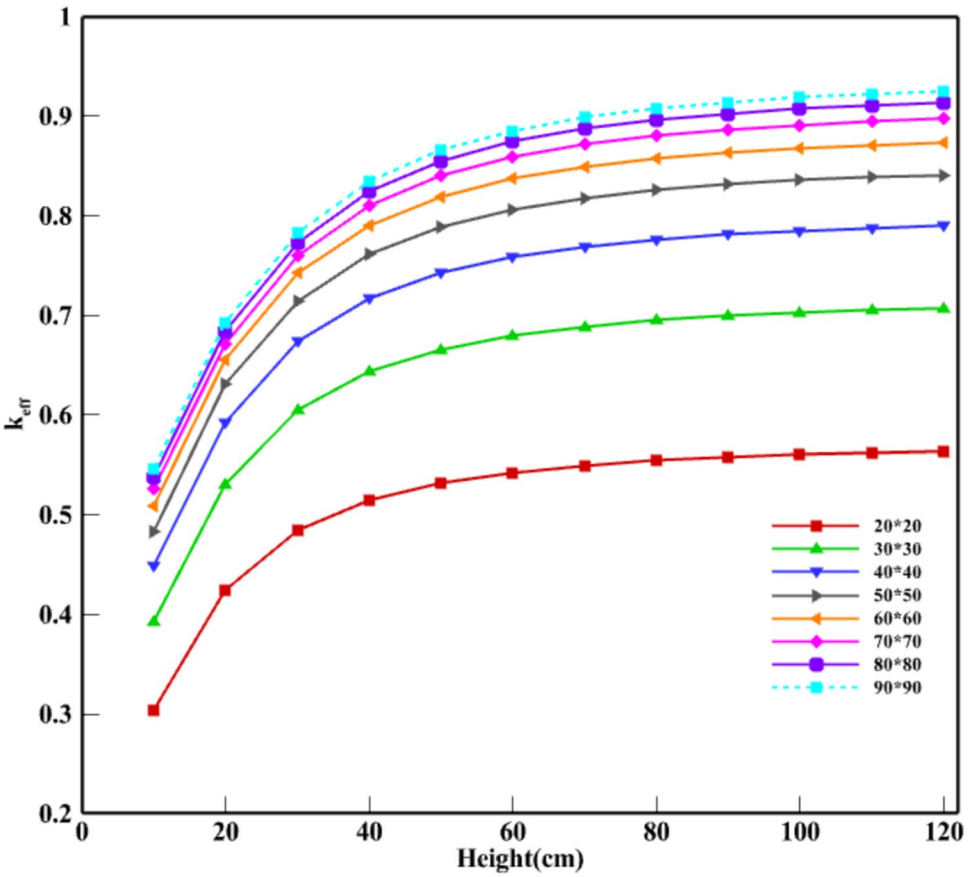

Fig. 5 (Color online) k_{eff} versus core height for different core arrangements of a deeply subcritical reactor

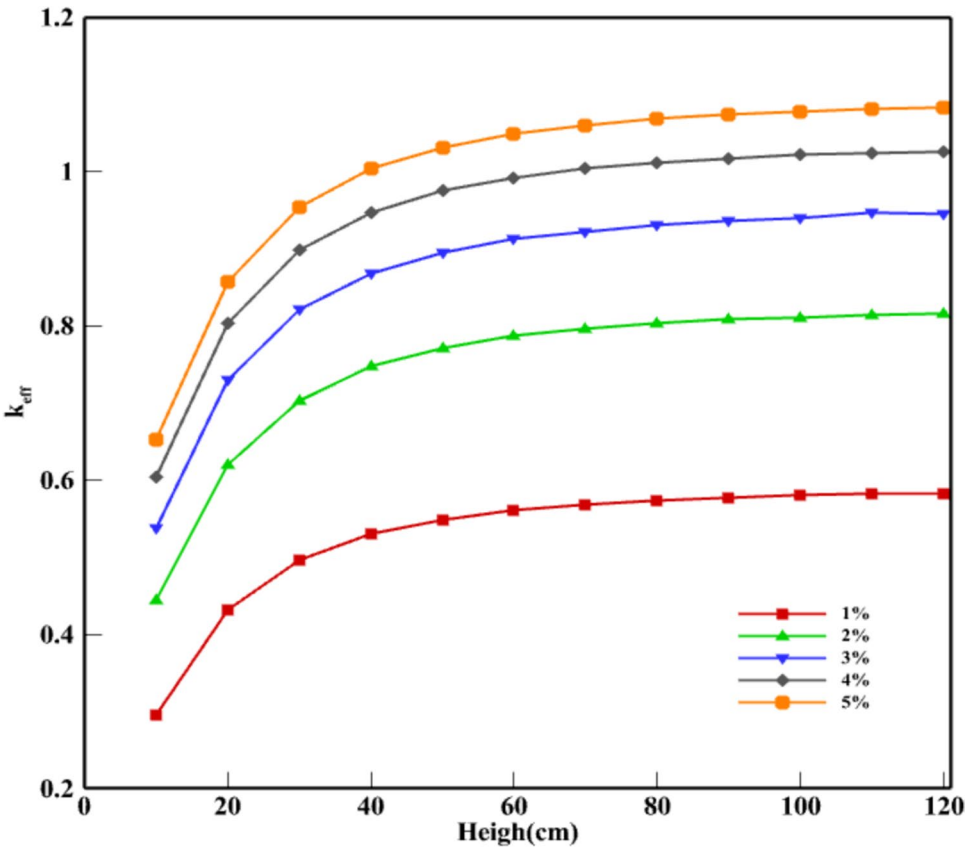

Fig. 6 (Color online) Effective multiplication factor in terms of core height for fuel enrichment between 1 and 5 wt% ^{235}U

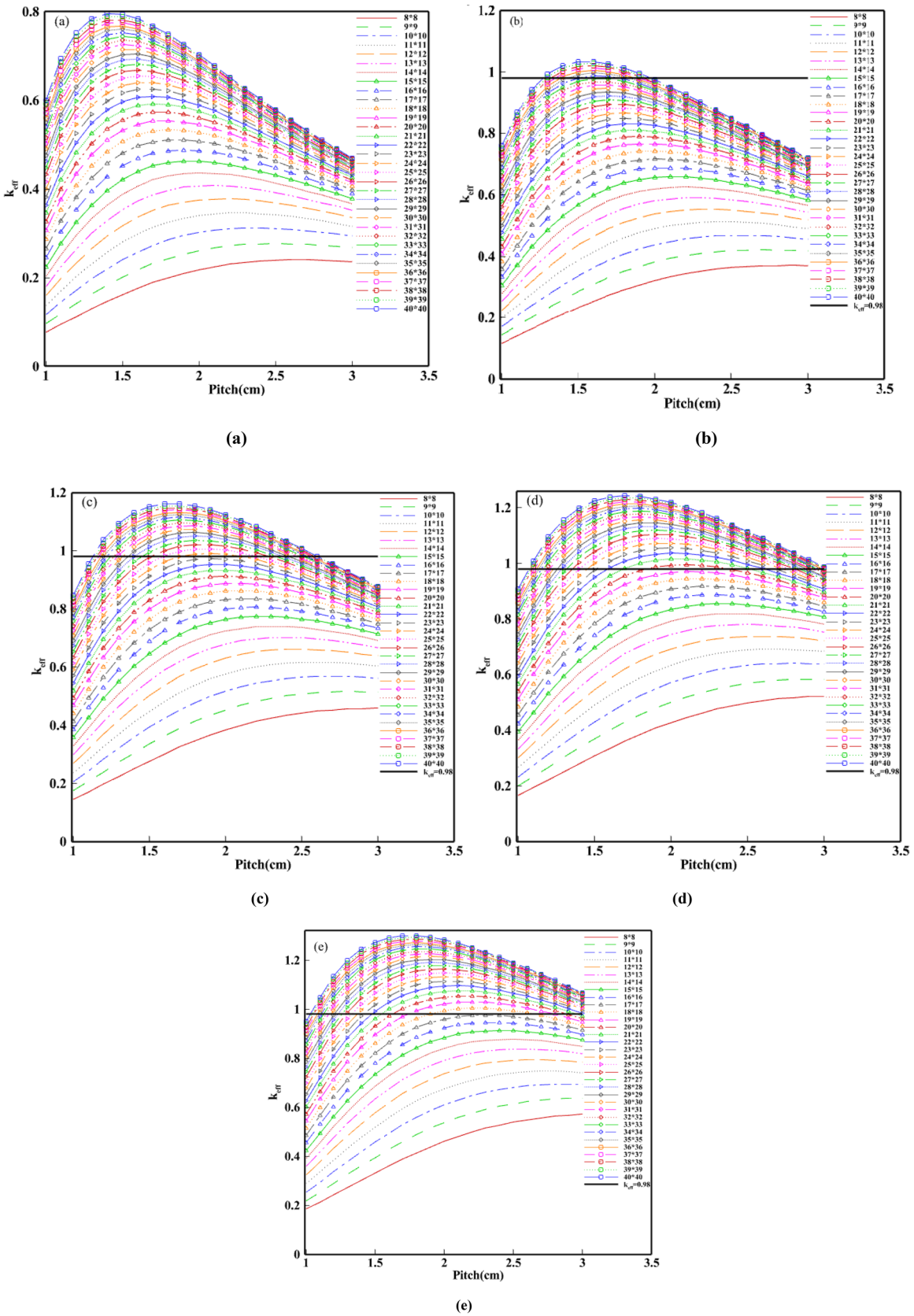

Fig. 7 (Color online) The k_{eff} versus core lattice pitch for different fuel enrichments: **a** 1% wt% of ^{235}U, **b** 2% wt% of ^{235}U, **c** 3% wt% of ^{235}U, **d** 4% wt% of ^{235}U, and **e** 5% wt% of ^{235}U

rods. As an example, the results of the enrichment of 1, 2, 3, 4, and 5% are shown in Fig. 7. As mentioned previously, an increase in the number of fuel rods leads to an increase in the effective multiplication factor, although the amount of this increase decreases with the number of fuel rods. For a constant enrichment, the optimal lattice pitch decreased as the number of fuel rods increased. By comparing Figs. 6e and 7a, it can be concluded that the optimal pitch increases with increasing fuel enrichment.

The optimal configurations and lattice pitches of the enriched subcritical cores, which lead to a k_{eff} below 0.98, are listed in Table 4. It can be observed that the number of fuel rods decreased with increasing fuel enrichment. However, the optimal pitch increased with increasing fuel enrichment. For example, the reactor will be permanently in a subcritical state if 361 conventional PWR fuel rods with an enrichment of 4 wt% ^{235}U are arranged in the reactor core.

3.4 Determination of the temperature coefficient

The determination of the negative temperature coefficient in thermal reactors is necessary to ensure safety. Therefore, the changes in the multiplication factor and temperature coefficient of reactivity with respect to the moderator and fuel temperature for 1–5 wt%^{235}U enrichment are presented in Figs. 8 and 9, respectively. It is worth to mention that the results of Figs. 8 and 9 are obtained based on the optimal configurations presented in Table 4. Therefore, the variation in the slope of the curves in Figs. 8 and 9 is mainly due to the variation in the optimal configurations. From a safety perspective, it is important to note that the k_{eff} decreases with increasing fuel or moderator temperature for all core configurations.

Table 4 The fuel rods arrangement based on fuel enrichment to design of a permanently subcritical reactor

Fuel enrichment (%)	Fuel rods arrangement	Number of fuel rods	Optimal pitch	$k_{eff,\ max}$
1	80×80	6400	1.3	0.913
1.2	80×80	6400	1.3	0.979
1.4	54×54	2116	1.4	0.979
1.6	43×43	1849	1.5	0.977
1.8	37×37	1369	1.6	0.977
2	33×33	1089	1.6	0.978
2.2	30×30	900	1.7	0.978
2.4	27×27	625	1.8	0.967
2.6	26×26	676	1.8	0.978
2.8	23×23	529	1.9	0.952
3	22×22	484	1.9	0.953
3.2	22×22	484	2	0.972
3.4	21×21	441	2.1	0.961
3.6	20×20	400	2.1	0.964
3.8	20×20	400	2.1	0.979
4	19×19	361	2.1	0.970
4.2	18×18	324	2.2	0.958
4.4	18×18	324	2.2	0.971
4.6	17×17	289	2.3	0.955
4.8	17×17	289	2.3	0.966
5	17×17	289	2.3	0.976

The moderator temperature coefficient (MTC) and the fuel temperature coefficient (FTC) values in different temperature ranges for 1–5 wt%^{235}U enrichment are demonstrated in Tables 5 and 6, respectively. In addition, the overall average MTC and FTC values are tabulated in these tables. According to the data in Table 5, the absolute value of MTC increases with increasing temperature at a constant enrichment. Conversely, Table 6 shows that the absolute value of FTC decreases with increasing temperature at a constant enrichment. Furthermore, the average MTC value varies between 8.5 and 14.5 pcm/K for different fuel enrichments. Moreover, the average value of FTC decreases between 0.865 and 2.711 pcm/K with increasing fuel enrichment from 1% to 5 wt%^{235}U. It can be concluded that the FTC value is related to fuel enrichment and is independent of the core arrangement, although the MTC value depends on both enrichment and core arrangement. The moderator and fuel temperature coefficients of reactivity were negative for all operational temperatures, ensuring the safety of the reactor. In addition, according to Figs. 8 and 9 and Tables 5 and 6, it can be concluded that the selected fuel assemblies remain in a subcritical state at all operational temperatures.

4 Conclusion

Subcritical research reactors are low-cost nuclear facilities and are a good choice for countries to develop nuclear infrastructure. In this study, two types of subcritical cores were introduced using the coupling of cell calculations of the DRAGON lattice code and core calculations of the DONJON code. The validity of the applied model was confirmed by the experimental results of Isfahan LWSCR, with relative errors of less than 0.24 and 4.1 for the effective multiplication factor and average reactivity coefficient, respectively. In the first step, a deeply subcritical reactor (k_{∞} is less than

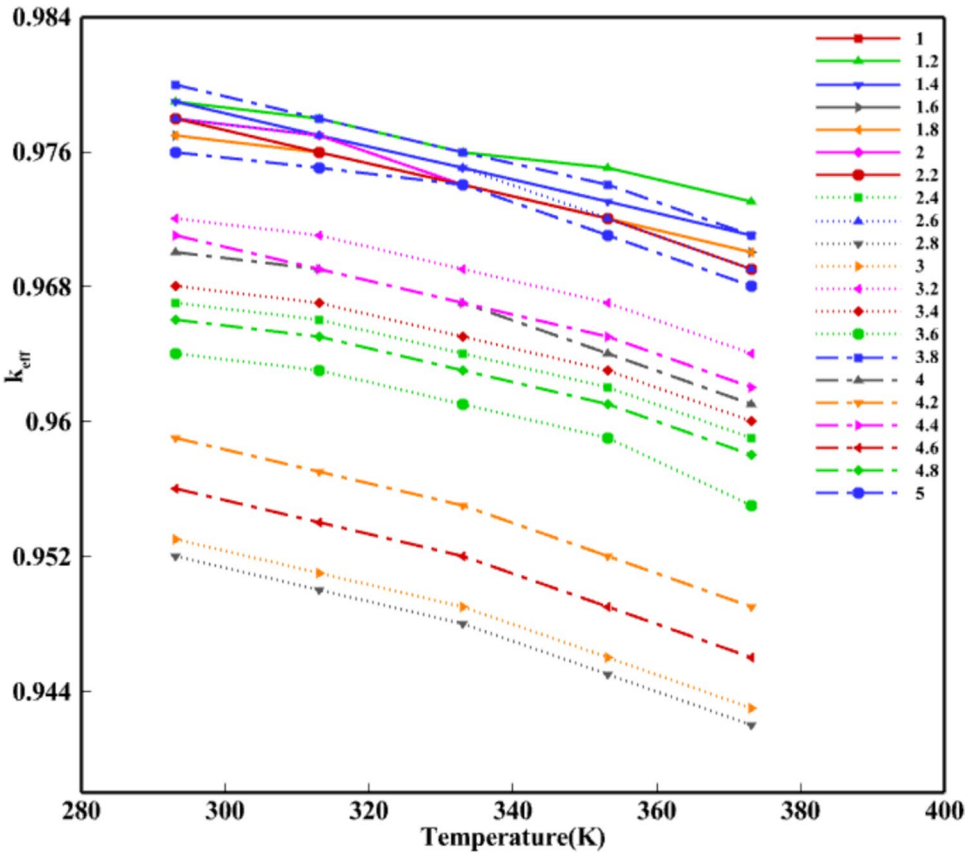

Fig. 8 (Color online) The effect of the moderator temperature changes on the k_{eff} for different fuel enrichments

unity) was designed using a core with an active length of 60 cm consisting of 80 × 80 fuel rods with 0.9 wt % of ^{235}U, which led to a maximum k_{eff} of 0.874 in the optimal lattice pitch of 1.3 cm. In the second step, the optimal subcritical core configurations for 1–5 wt%^{235}U that led to k_{eff} of less than 0.98 were introduced. Furthermore, the fuel and moderator temperature coefficients were calculated to ensure that the designed assemblies remained in a subcritical state for all operational temperatures. The FTC value was found to be related to fuel enrichment and independent of core configuration, although the MTC value depended on both enrichment and core configuration. The results show that the designed subcritical core configurations are safe at all operational temperatures. The results of this study can be applied to the design of subcritical reactors that use PWR commercial fuel.

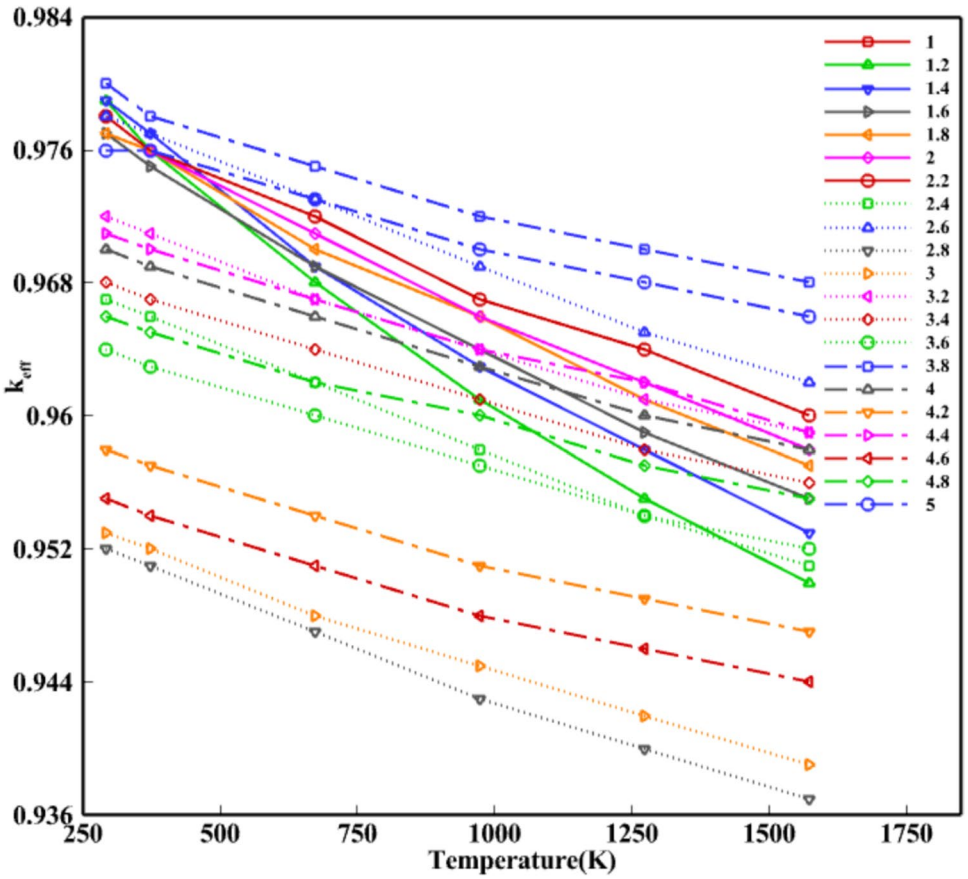

Fig. 9 (Color online) Effect of fuel temperature changes on the k_{eff} for different fuel enrichments

Table 5 Effect of the moderator temperature changes on MTC for different fuel enrichments

Enrichment (%)	$\alpha_{293-313\,\text{K}}(\frac{\text{pcm}}{\text{K}})$	$\alpha_{313-333\,\text{K}}(\frac{\text{pcm}}{\text{K}})$	$\alpha_{333-353\,\text{K}}(\frac{\text{pcm}}{\text{K}})$	$\alpha_{353-373\,\text{K}}(\frac{\text{pcm}}{\text{K}})$	$\alpha_{\text{Average}}(\frac{\text{pcm}}{\text{K}})$
1	− 6.984	− 8.144	− 10.741	− 10.991	− 9.215
1.2	− 7.133	− 7.714	− 8.758	− 10.592	− 8.549
1.4	− 6.956	− 9.479	− 9.992	− 11.087	− 9.378
1.6	− 7.446	− 9.238	− 11.025	− 12.247	− 9.989
1.8	− 6.846	− 9.432	− 11.173	− 12.685	− 10.034
2	− 7.915	− 11.593	− 13.285	− 15.250	− 12.011
2.2	− 7.983	− 11.100	− 11.806	− 16.153	− 11.761
2.4	− 7.374	− 11.111	− 12.386	− 15.968	− 11.710
2.6	− 7.741	− 11.773	− 13.256	− 16.260	− 12.258
2.8	− 8.634	− 12.730	− 14.443	− 18.474	− 13.570
3	− 9.625	− 12.557	− 16.084	− 19.738	− 14.501
3.2	− 6.636	− 9.969	− 13.365	− 15.852	− 11.456
3.4	− 6.579	− 8.275	− 12.633	− 14.088	− 10.394
3.6	− 7.203	− 10.144	− 13.117	− 16.796	− 11.815
3.8	− 5.849	− 10.281	− 12.505	− 16.992	− 11.407
4	− 6.489	− 11.406	− 14.606	− 17.930	− 12.608
4.2	− 6.897	− 10.603	− 13.981	− 17.442	− 12.231
4.4	− 6.670	− 8.950	− 14.763	− 16.506	− 11.722
4.6	− 6.782	− 8.998	− 13.676	− 17.223	− 11.670
4.8	− 4.755	− 9.547	− 12.597	− 16.793	− 10.923
5	− 5.063	− 8.551	− 12.915	− 15.666	− 10.549

Table 6 Effect of changing the moderator temperature on FTC for different fuel enrichments

Enrichment (%)	$\alpha_{293-373\,K}$ ($\frac{pcm}{K}$)	$\alpha_{373-673\,K}$ ($\frac{pcm}{K}$)	$\alpha_{673-973\,K}$ ($\frac{pcm}{K}$)	$\alpha_{973-1273\,K}$ ($\frac{pcm}{K}$)	$\alpha_{1273-1573\,K}$ ($\frac{pcm}{K}$)	$\alpha_{Average}$ ($\frac{pcm}{K}$)
1	−3.789	−3.133	−2.715	−2.399	−2.185	−2.711
1.2	−3.727	−2.927	−2.431	−2.189	−1.988	−2.468
1.4	−2.941	−2.543	−2.116	−1.861	−1.740	−2.120
1.6	−2.549	−2.250	−1.876	−1.677	−1.507	−1.873
1.8	−2.227	−1.982	−1.642	−1.552	−1.388	−1.678
2	−2.246	−1.920	−1.658	−1.455	−1.350	−1.637
2.2	−2.016	−1.721	−1.498	−1.335	−1.244	−1.485
2.4	−1.898	−1.608	−1.354	−1.263	−1.144	−1.377
2.6	−1.859	−1.535	−1.390	−1.147	−1.131	−1.336
2.8	−1.650	−1.534	−1.251	−1.132	−1.078	−1.274
3	−1.805	−1.422	−1.249	−1.121	−1.022	−1.241
3.2	−1.524	−1.289	−1.139	−1.031	−0.995	−1.139
3.4	−1.527	−1.260	−1.038	−0.990	−0.861	−1.068
3.6	−1.526	−1.200	−1.088	−0.943	−0.915	−1.067
3.8	−1.473	−1.178	−0.964	−0.963	−0.841	−1.017
4	−1.327	−1.123	−1.053	−0.932	−0.836	−1.007
4.2	−1.325	−1.136	−0.988	−0.849	−0.783	−0.963
4.4	−1.294	−1.109	−0.916	−0.835	−0.805	−0.940
4.6	−1.382	−1.040	−0.902	−0.836	−0.770	−0.918
4.8	−1.140	−1.017	−0.887	−0.774	−0.738	−0.872
5	−1.125	−0.989	−0.867	−0.813	−0.723	−0.865

Author contributions All authors contributed to the study conception and design. Material preparation, data collection, and analysis were performed by S. Abedi, J. Mokhtari, and M. H. Choopan Dastjerdi. The first draft of the manuscript was written by S. Abedi and J. Mokhtari, and all authors commented on previous versions of the manuscript. All authors read and approved the final manuscript.

Declarations

Conflict of interest The authors declare that they have no competing interests.

References

1. J. Rataj, F. Fejt, J. Frýbort et al., The project of VR-2 subcritical assembly. Nucl. Eng. Des. **386**, 111578 (2022). https://doi.org/10.1016/j.nucengdes.2021.111578
2. I. Jarrah, S. Malkawi, M.I. Radaideh et al., Experimental validation of the neutronic parameters in the Jordan subcritical assembly. Prog. Nucl. Energ. **108**, 71–80 (2018). https://doi.org/10.1016/j.pnucene.2018.04.014
3. R.D.E. Gatchalian, P.V. Tsvetkov, Reactor physics analysis of a source-driven TRIGA configuration in subcritical domain. Ann. Nucl. Energy **186**, 109787 (2023). https://doi.org/10.1016/j.anucene.2023.109787
4. A. Asuncion-Astronomo, Z. Štancar, T. Goričanec et al., Computational design and characterization of a subcritical reactor assembly with TRIGA fuel. Nucl. Eng. Technol. **51**(2), 337–344 (2019). https://doi.org/10.1016/j.net.2018.09.025
5. L.H. Pardo, D.M. Pérez, D.E.M. Lorenzo et al., Coupled multiphysics simulation for the evaluation of an accelerator-driven Aqueous Homogeneous Subcritical System for medical isotope production. Prog. Nucl. Energy **134**, 103692 (2021). https://doi.org/10.1016/j.pnucene.2021.103692
6. N. Manwaring, R.A. Borrelli, At-power subcritical multiplication in the advanced test reactor. Nucl. Eng. Des. **401**, 112040 (2023). https://doi.org/10.1016/j.nucengdes.2022.112040
7. Z.I. Zafar, M.H. Kim, Embedded fission source approach to analyze external source effect in a subcritical reactor. Nucl. Eng. Des. **327**, 238–247 (2018). https://doi.org/10.1016/j.nucengdes.2017.11.039
8. L. Taghizadeh, A. Zolfaghari, M. Zangian et al., Comparison of probabilistic and deterministic methods for calculation of kinetic parameters of HWZPR. Ann. Nucl. Energy **165**, 108633 (2022). https://doi.org/10.1016/j.anucene.2021.108633
9. P. Kaviani, J. Mokhtari, S.M. Mirvakili, Integral form of the control rod calibration curve in the new core configuration of HWZPR using rod insertion method. Prog. Nucl. Energ. **125**, 103375 (2020). https://doi.org/10.1016/j.pnucene.2020.103375
10. A. Asgari, M.H.C. Dastjerdi, J. Mokhtari, A computational-experimental model of reactor kinetic for investigating the linearity response of in-core neutron detectors of a low power research reactor. Nucl. Eng. Des. **424**, 113242 (2024). https://doi.org/10.1016/j.nucengdes.2024.113242
11. A. Asgari, S.A. Hosseini, M.H.C. Dastjerdi et al., Determination of the linear behavior of FC detectors in Isfahan MNSR using ex-core offline and online experiments. Nucl. Eng. Des. **415**, 112681 (2023). https://doi.org/10.1016/j.nucengdes.2023.112681
12. B. Jandaghian, J. Mokhtari, M.C. Dastjerdi, Design and simulation of neutron radiography system for an aqueous homogeneous solution reactor. Prog. Nucl. Energ. **173**, 105229 (2024). https://doi.org/10.1016/j.pnucene.2024.105229
13. M. Jafari, H. Jafari, M.C. Dastjerdi et al., Designing a system of boron concentration measurement in solution samples by the

PGNAA facility of the Isfahan MNSR reactor. Nucl. Eng. Des. **416**, 112782 (2024). https://doi.org/10.1016/j.nucengdes.2023.112782
14. Y. Abbassi, J. Mokhtari, S.M. Mirvakili et al., Adoption of a fast dynamic model to simulate transient operations of MNSR. Nucl. Eng. Des. **421**, 113118 (2024). https://doi.org/10.1016/j.nucengdes.2024.113118
15. Z. Gholamzadeh, E. Bavarnegin, R. Ebrahimzadeh et al., Experimental evaluation of transition rate of sapphire crystal for thermal and fast neutrons using MNSR vertical neutron beam line. Heliyon **10**, e24160 (2024). https://doi.org/10.1016/j.heliyon.2024.e24160
16. J. Mokhtari, M.C. Dastjerdi, B. Soleimani, Improvement of the quality of neutron radiography beamlines in Isfahan MNSR. Nucl. Instrum. Meta. A **1056**, 168660 (2023). https://doi.org/10.1016/j.nima.2023.168660
17. A. Asgari, S.A. Hosseini, M.H.C. Dastjerdi et al., Determination of the neutron scattering contribution in a neutron calibration field based on MNSR. Nucl. Instrum. Methods Phys. Res. Sect. A Accel. Spectrom. Detect. Assoc. Equip. **1061**, 169154 (2024). https://doi.org/10.1016/j.nima.2024.169154
18. M.C. Dastjerdi, J. Mokhtari, M. Toghyani, Design, construction, and characterization of a prompt gamma neutron activation analysis (PGNAA) system at Isfahan MNSR. Nucl. Eng. Technol. **55**(12), 4329–4334 (2023). https://doi.org/10.1016/j.net.2023.08.013
19. B. Jandaghian, M.C. Dastjerdi, J. Mokhtari, Characterization of neutronic parameters and radiation shielding design for an aqueous homogeneous reactor. Nucl. Eng. Des. **417**, 112832 (2024). https://doi.org/10.1016/j.nucengdes.2023.112832
20. E. Teimoory, M.A. Allaf, J. Mokhtari et al., Development and characterization of fission chamber neutron detectors in Isfahan miniature neutron source reactor. Radiat. Phys. Chem. **215**, 111360 (2024). https://doi.org/10.1016/j.radphyschem.2023.111360
21. R. Pourimani, M.H.C. Dastjerdi, E.H. Farahani et al., Measurements of concentrations of some elements in the meat and skin of farmed and marine fish of the Persian Gulf using the neutron activation analysis technique. Eur. Phys. J. Plus **139**(6), 552 (2024). https://doi.org/10.1140/epjp/s13360-024-05350-5
22. M. Bagherzadeh, M.C. Dastjerdi, J. Mokhtari, Feasibility study of nanomaterials synthesis at MNSR research reactor through design and construction of a gamma irradiation cell. Nucl. Eng. Des. **414**, 112621 (2023). https://doi.org/10.1016/j.nucengdes.2023.112621
23. M.C. Dastjerdi, J. Mokhtari, M. Toghyani et al., Feasibility study on PGNAA experiments using a prototype neutron beam at Isfahan MNSR. J. Instrum. **18**(07), P07031 (2023). https://doi.org/10.1088/1748-0221/18/07/P07031
24. M. Bagherzadeh, M. Karimi, M.H. Choopan Dastjerdi et al., Long-time irradiation effect on corrosion behavior of aluminum alloy in pool water of low-power research reactor. Sci. Rep. **13**(1), 17007 (2023). https://doi.org/10.1038/s41598-023-44287-0
25. Z. Gholamzadeh, R. Ebrahimzadeh, M.H. Choopan Dastjerdi et al., Assessment of shielding performance of NBR through simulation and experiments at MNSR beam line. Radiat. Phys. Eng. (2024). https://doi.org/10.22034/rpe.2024.420403.1167
26. Z. Zhang, T. Wu, Y. Wang et al., Core design and neutronic study on small reactor with advanced fuel designs. Nucl. Mater. Energ. **29**, 101068 (2021). https://doi.org/10.1016/j.nme.2021.101068
27. J.Z. Liu, S. Miwa, H. Karasawa et al., Effect of molybdenum release on UO2/MOX fuel oxidation under severe light water reactor accident conditions. Nucl. Mater. Energ. **37**, 101532 (2023). https://doi.org/10.1016/j.nme.2023.101532
28. F. Liu, W. Zhang, B. Liu et al., Fuel depletion characteristics of MA transmutation in PWR. Nucl. Mater. Energ. **30**, 101119 (2022). https://doi.org/10.1016/j.nme.2022.101119
29. Y. Abbassi, S.M. Mirvakili, J. Mokhtari, Development of a fast thermal-hydraulic model to simulate heat and fluid flow in MNSR. Ann. Nucl. Energy **178**, 109371 (2022). https://doi.org/10.1016/j.anucene.2022.109371
30. M.H. Rabir, A.F. Ismail, M.S. Yahya, Neutronics calculation of the conceptual TRISO duplex fuel rod design. Nucl. Mater. Energy **27**, 101005 (2021). https://doi.org/10.1016/j.nme.2021.101005
31. S. Chen, C. Yuan, Neutronic study of UO2-BeO fuel with various claddings. Nucl. Mater. Energy **22**, 100728 (2020). https://doi.org/10.1016/j.nme.2020.100728
32. H. R. Vega Carrillo, Subcritical Nuclear Assembly, (2014)
33. M. Al-Dbissi, L. Khalayleh, E. Smadi, Neutronic characterization of the Jordanian Subcritical Assembly (JSA) using Monte Carlo N-particle code. (2017)
34. M.I. Radaideh, I. Jarrah, S. Malkawi et al., Reactivity and flux characterization of the Jordan subcritical assembly. Prog. Nucl. Energy **108**, 43–53 (2018). https://doi.org/10.1016/j.pnucene.2018.05.003
35. A. Polanski, S. Petrochenkov, V. Shvetsov et al., Power upgrade of the subcritical assembly in Dubna (SAD) to 100 kW. Nucl. Instrum. Methods Phys. Res. A **562**(2), 879–882 (2006). https://doi.org/10.1016/j.nima.2006.02.080
36. Z. Nasr, M. Iravani, J. Mokhtari, Measurement of Isfahan heavy water zero-power reactor kinetic parameters using advanced pulsed neutron source method in a near critical state. Appl. Radiat. Isot. **204**, 111126 (2024). https://doi.org/10.1016/j.apradiso.2023.111126
37. IAEA-TECDOC-1976, Considerations of Safety and Utilization of Subcritical Assemblies (1976)
38. S. Kamalpour, H. Khalafi, S.M. Mirvakili, Conceptual design study of light water subcritical assembly. Prog. Nucl. Energ. **73**, 107–112 (2014). https://doi.org/10.1016/j.pnucene.2014.01.012
39. Safety Analysis Report of Isfahan LWSCR, NSTRI, (2023)
40. C.M. Persson, P. Seltborg, A. Ahlander et al., Analysis of reactivity determination methods in the subcritical experiment yalina. Nucl. Instrum. Methods Phys. Res. A. **554**(1), 374–383 (2005). https://doi.org/10.1016/j.nima.2005.07.058
41. A. Hébert, DRAGON5 and DONJON5, the contribution of École polytechnique de Montréal to the SALOME platform. Ann. Nucl. Energy **87**, 12–20 (2016). https://doi.org/10.1016/j.anucene.2015.02.033
42. A. Talamo, Y. Gohar, Deterministic and Monte Carlo modeling and analyses of YALINA-THERMAL subcritical assembly (No. ANL-NE-10/17). Argonne National Lab. (ANL), Argonne, IL (United States), (2010)
43. X. Yang, G. Shi, K. Wang, Benchmark validation of DRAGON program using WIMS-D nuclear data library. Nuclear Power Eng. **28**, 20 (2007). (**in Chinese**)
44. Z. Zhao, Y. Guo, Y. Zou et al., Validation and application of the DRAGON5 lattice code for neutronics and burnup analysis of VVER-1000 pin cell and assembly model. Nucl. Eng. Des. **407**, 112279 (2023). https://doi.org/10.1016/j.nucengdes.2023.112279
45. L. Liponi, Calculation and verification of assembly discontinuity factors for the DRAGON/PARCS code sequence. Ecole Polytechnique, Montreal (Canada), (2017)
46. Z. Ni, J. Xie, M.A. Wasaye et al., Effect of higher-order harmonics on the steady-state neutron flux in accelerator-driven subcritical reactors. Int. J. Energ. Res. **2023**, 4114886 (2023). https://doi.org/10.1155/2023/4114886
47. H. El Yaakoubi, H. Boukhal, T. El Bardouni et al., Validation study of the reactor physics lattice transport code DRAGON5 & the Monte Carlo code OpenMC by critical experiments of light water reactors. J. King Saud Univ. Sci. **31**(4), 1271–1275 (2019). https://doi.org/10.1016/j.jksus.2019.02.004

48. A. Talamo, Y. Gohar, G. Aliberti et al., Deterministic analyses of YALINA-thermal subcritical assembly with DRAGON-PARTISN software. In International Topical Meeting on Nuclear Research Applications and Utilization of Accelerators. (2009)
49. S. Pino-Medina, J.L. François, Neutronic analysis of the NuScale core using accident tolerant fuels with different coating materials. Nucl. Eng. Des. **377**, 111169 (2021). https://doi.org/10.1016/j.nucengdes.2021.111169
50. H. El Yaakoubi, H. Boukhal, T. El Bardouni et al., Neutronic study of the 2-MW TRIGA MARK-II research reactor by the deterministic codes DRAGON5 & DONJON5. Appl. Radiat. Isot. **157**, 109026 (2020). https://doi.org/10.1016/j.apradiso.2019.109026
51. S. Banerjee, T. Singh, Study of PHWR and BWR lattice benchmark problems with multigroup multidimensional neutron transport code DRAGON. Life Cycle Reliab. Saf. Eng. **9**, 13–43 (2020). https://doi.org/10.1007/s41872-019-00108-w